Current Journal of Applied Science and Technology

39(33): 35-46, 2020; Article no.CJAST.62159
ISSN: 2457-1024
(Past name: British Journal of Applied Science & Technology, Past ISSN: 2231-0843, NLM ID: 101664541)

Topology Optimization of a Straight Subsoiler through Computer Mathematical Modelling

Saqib Parvaze Allaie[1*], Ashok Tripathi[1], P. M. Dsouza[1] and Sabah Parvaze[2]

[1]Department of Farm Machinery and Power Engineering, VIAET, SHUATS, Prayagraj, UP, India.
[2]College of Agricultural Engineering and Technology, SKUAST-K, Shalimar, J&K, India.

Authors' contributions

This work was carried out in collaboration with all the authors. Author SPA designed the study, performed the statistical analysis, wrote the protocol and wrote the manuscript's first draft. Authors AT and PMD managed the analyses and verification of the study. Author SP managed the literature searches. All authors read and approved the final manuscript.

Article Information

DOI: 10.9734/CJAST/2020/v39i3331016
Editor(s):
(1) Samir Kumar Bandyopadhyay, University of Calcutta, India.
(2) Dr. Jakub Kostecki, University of Zielona Góra, Poland.
Reviewers:
(1) Gonçalo Renildo Lima Cerqueira, Universidade Estadual Do Sudoeste Da Bahia, Brazil.
(2) Waheed Yosry Ali, Minia University, Egypt.
Complete Peer review History: http://www.sdiarticle4.com/review-history/62159

Original Research Article

Received 14 August 2020
Accepted 18 October 2020
Published 30 October 2020

ABSTRACT

Technologies and computer programs available today provide us with design programs and analytical techniques for solving complex problems in the different engineering disciplines. These technologies and programs have also found their significance in agricultural research. Computer-aided mathematical modelling was used for carrying out the design optimization of a straight subsoiler. At the initial stage, the static structural analysis under static loading conditions was performed. Details on the material and dimensions for the subsoiler were acquired from the manufacturer at the regional level. The existing subsoiler was then optimized for shank thickness, curve length, and shank width. Optimization was carried out for the objectives seeking minimum solid mass and maximum safety factor. The optimized design obtained was remodeled, and its static analysis performed. Results of the stresses, deformation, and safety factor before and after optimization were compared, and the conclusions drawn. The static structural analysis revealed that before optimization, the subsoiler mass was 24.54 kg, and the volume was 3117701.77 mm^3. The maximum total deformation was 4.959 mm, maximum equivalent stress was 270.09 MPa, and the maximum principal stress was 295.06 MPa. The minimum value for the safety factor was 1.296.

**Corresponding author: E-mail: saqibparvaze@gmail.com;*

Parametric correlation of the input and output parameters showed that the relationship among two input parameters viz. shank thickness, shank width, and output parameters was strong. These input parameters were used for response surface generation and design optimization. Optimization reduced both the subsoiler mass and volume by 14.86 %. The maximum equivalent stress and maximum principal stress reduced by 4.10% and 5.39%, respectively, while the total deformation, minimum safety factor, and maximum working life increased by 7.15%, 4.28%, and 14.26%, respectively.

Keywords: Subsoiler; computer-aided design; finite element method; structural optimization; agricultural machinery design; straight subsoiler.

1. INTRODUCTION

Crops cultivated within controlled conditions require a certain number of critical factors concerning the soil structure, including adequate space for root growth, a sufficient amount of organic matter distribution, and plenty of water permeability. Therefore, the soil is required to be well prepared for the crops by tillage before seeding. However, each year, the soil in agricultural areas gets more compacted (around 250 mm) because of the repetition of tillage practices and traffic movement in the field [1]. Soil compaction leads to denser soil, small-sized pores, and increased soil strength [2,3]. As a result, root emergence along with the air and water movement inside the soil is restricted, and eventually, the yield is lowered [4,5].

One of the useful approaches for avoiding the adverse effects of soil compaction in agricultural regions is the subsoiling operation [6,7]. Subsoiling can help alleviate the complications created by soil compaction by reducing the soil strength and improving the conditions for better crop production [8,9]. Subsoiling is carried out by equipment known as a subsoiler. The subsoiler's working principle is similar to that of a chisel plow, but its construction is heavier and rigid as it is required to operate at depths of about 90 cm for breaking up the deep soil layers. Subsoiling is a very heavy-duty operation and requires a high draft and mechanical energy [10,11]. Subsoilers are typically manufactured as steel structures comprising the main framework, narrow share, and support parts. During its working, various reaction forces from the soil act on the subsoiler because of the deep tillage operation [12]. If the subsoiler construction cannot compensate for the soil's reaction forces, the subsoiler elements get deformed. These deformations can further contribute to machinery failure during operation [13].

Therefore, the effect of different forces and the resulting stress distribution must be determined precisely to prevent the subsoilers breakdown during operation. Such information is of utmost importance for the machine designer and manufacturers. The machine manufacturer uses specific materials only during the manufacturing process to reduce possible errors and corresponding failures. These materials have high safety coefficients or higher component weights. However, the selection of such materials renders the equipment safe but results in higher overall weights and high production costs. Several working designs could be satisfied within the operating conditions, but the goal is to obtain an optimum design. Using optimization techniques is thus an essential application for the machine industries [14]. The software-based integrated numerical methods and optimization techniques have been used for machine design procedures since the 1960s. Keeping in focus the system for machine optimization, the structural optimization of the machine becomes a necessity. Structural optimization aims to obtain an optimum structural framework using the geometric, material, and topological parameters [15,16].

Developing a global model is impractical due to the complex conditions of the operating environment. Jayasurya and Salokhe (2001) [17] recommended applying computer-aided modeling for setting up supporting databases for the model specifications to employ them for specific conditions or machinery design. Computer-aided design programs help set up a complete system of design processes, particularly the three-dimensional modeling (3D) and finite element analysis (FEA) programs [18,19]. Applying these methods for designing agricultural machines is inevitable nowadays [20,21].

The current study was undertaken, keeping in view the optimization of an existing tillage tool. The 3D modeling, FEA, and structural analysis for a straight subsoiler manufactured by a local manufacturer were performed. The study aimed to obtain the optimum design parameters of the subsoiler system with minimum weight. Advanced computer-aided modeling (CAM) techniques were utilized for achieving the goals of the study within the defined objective functions and design constraints.

2. METHODOLOGY

The 3D model of the subsoiler was first created using SolidWorks software. The model was attached to the ANSYS analysis system, and its structural analysis was performed. Design optimization was followed under the conditions of fixed boundary. Optimization for three parameters – shank thickness, curve length, and shank width was carried out. Details on the material and dimensions for the subsoiler were acquired from the manufacturer at the regional level. The obtained optimized design was remodeled, and static structural analysis performed. Results before and after optimization were compared, and the conclusions drawn.

2.1 Model Building

A 3D solid model for the subsoiler was created using SolidWorks 2016 software. SolidWorks is a feature-based, history-based, associative, parametric 3D CAD program. It is used for mechanical design automation applications. SolidWorks models comprise 3D geometries specifying the edges, faces, and surfaces. The model was first made as a 2D sketch and then converted to a 3D model in SolidWorks. Also, the parameters for optimization were given different names to import them into ANSYS Workbench. The parameter names have a prefix "DS_" as ANSYS recognizes parameters with specific prefixes only [22]. If the prefix is not provided, ANSYS does not import the same.

2.2 Static Structural Analysis

Static structural analysis and optimization were carried out in the ANSYS Workbench. The structural analysis defines the displacements, forces, stresses, and strains in the structure [23]. 3D model generated from SolidWorks was imported to ANSYS and the material properties applied. The material for the subsoiler was hot-rolled structural steel [24]. The meshing process followed this. ANSYS meshing functions were utilized to generate a fine mesh of element size of 5 mm to obtain a quantitative analysis of higher accuracy (Fig. 1.). In the meshing process, the geometry is discretized spatially into smaller elements and nodes [25]. This meshing represents the mass distribution and stiffness of the structure mathematically [26].

The application of boundary conditions followed the meshing process. Boundary conditions are usually termed supports or loads. They restrict the model by applying forces or rotations or by

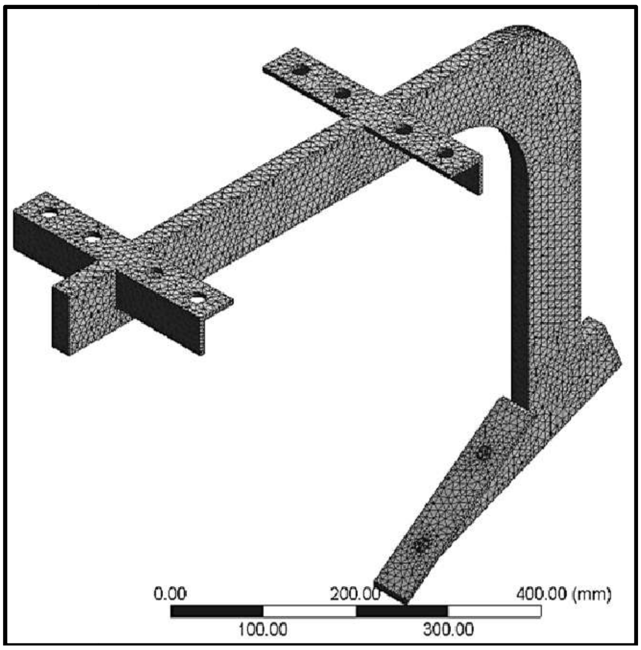

Fig. 1. Meshed straight subsoiler

securing the model to prevent its deformation [27]. The holes of the shank (
Fig.2.) that provide the facility of connecting the shank to the subsoiler frame were chosen as one boundary condition. The other boundary condition was the force on the subsoiler reversible blades (
Fig.3.). The force was taken as 7857 N [28].

After defining the boundary conditions, the simulation was carried out. The parameters selected for the simulation were Total Deformation, Equivalent stress, Maximum Principal Stress, and Factor of Safety. At this step, ANSYS passes its data to the solver, depending on the analysis type. The results obtained were exported along with the inputs as a set of parameters for further analysis.

The parametric set consists of different parameters. Parameters can be input or output parameters with their values numeric, non-numeric, or Boolean, connected to an application's data property models. The thickness of shank (P1), length of a curve (P2), and width of shank (P3) were the input parameters; and the parabolic subsoiler mass (P4), total deformation (P5), equivalent stress (P6), maximum principal stress (P7), safety factor (P8) and parabolic subsoiler volume (P9) were the output parameters.

2.3 Optimization

Optimization is defined as obtaining the solution for one variable that acts as a constraint for a set of variables that are the minimized functions of an objective function [13]. Structural optimization problems can be classified based upon the structure type, the structural variable design type, and the type of structural behavior. Structural optimization problems are primarily of three different classes, i.e., shape, sizing (mass), and topology, which depend on the structure type to be optimized [29]. The present study was devoted to the subsoiler's size optimization. This means that the mass must be minimum while restricting different stresses below the materials yield point.

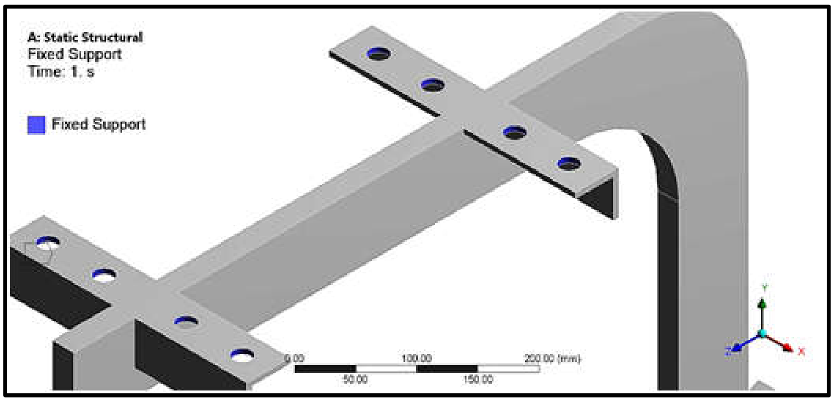

Fig. 2. Fixed support condition for the Straight subsoiler

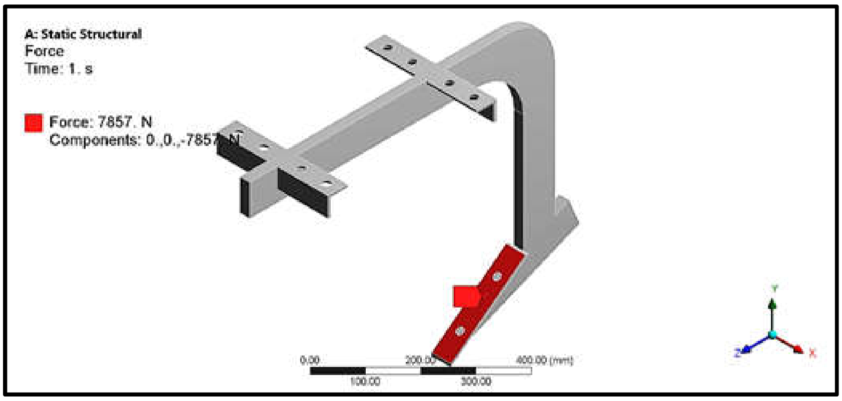

Fig. 3. Force condition for the Straight subsoiler

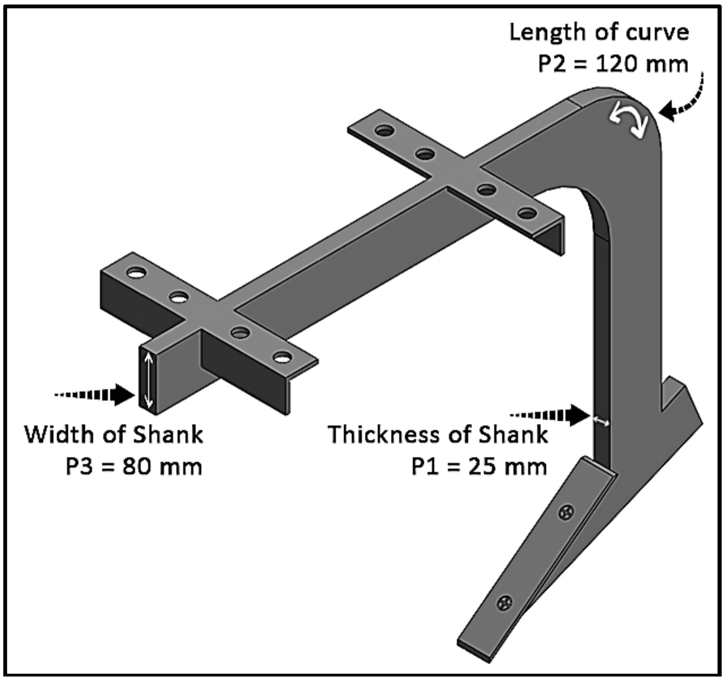

Fig. 4. Design parameters of the Straight subsoiler

For reducing the stress concentrations on the subsoiler shank, design enhancements of the shank have been suggested, limited to only three geometrical parameters – P1, P2, and P3. The output parameters included P4, P5, P6, P7, P8, and P9. The design constraints for the different design parameters were determined from the "What-if" analysis using ANSYS and are as follows:

P1: 20 mm ≤ P1 ≤ 25 mm
P2: 110 mm ≤ P2 ≤ 130 mm
P3: 70 mm ≤ P3 ≤ 90 mm

The ANSYS optimization module was employed in the optimization process. Optimization consists of three main steps – parametric correlation, response surface generation, and goal-driven optimization. Parametric correlation determines the effect of each input parameter on the various output parameters. Parametric correlation results were further used for the response surface system, including the design of experiments and response surface generation. The Design of Experiments (DOE) is a method used to find the position of sampling points. In the DOE, the highest correlation parameters were selected as the input parameters and the design points generated. The output of DOE is used for the generation of response surfaces. The response surfaces are functions of a distinct nature where the input parameters define the output parameters; developed from the DOE. Once response surfaces are created, it is possible to create and manage response points and charts [30].

Response surface generation was followed by Goal-Driven Optimization (GDO). GDO can be used to specify a sequence of design goals to produce an optimized design. One thousand sampling points were generated and organized to seek minimum solid mass and maximum safety factor (Table 1) [31]. A targeted design point corresponding to the optimal geometry was generated.

Table 1. Objectives and constraints definitions

Name	Objective	Constraint		
	Type	Type	Lower bound	Upper bound
Minimize P4; P4<=24.54 kg	Minimize	Values<=Upper Bound		24.54
Maximize P8; P8>=1.295	Maximize	Values>=Lower Bound	1.295	

2.4 Comparison

The target design geometry obtained post-optimization was used to generate the optimized design. 3D model of the subsoiler was created using the post-optimization design parameters and re-analyzed using ANSYS software. Results of the stresses, deformation, and safety factor before and after optimization were compared, and the conclusions drawn.

3. RESULTS AND DISCUSSION

3.1 Model Building

The 2D and 3D geometric views of the subsoiler are shown in Fig. 5.

3.2 Static Structural Analysis

Meshing the subsoiler produced 51247 nodes and 27135 elements. The total mass and volume were determined as 24.54 kg and 3117701.77 mm^3, respectively. The stresses, deformation, and safety factor from the structural analysis are given in Table 2.

Table 2. Output parameters from the structural analysis

Particulars	Minimum	
Total Deformation (maximum)	4.959	mm
Equivalent Stress (maximum)	270.090	MPa
Maximum Principal Stress (maximum)	295.060	MPa
Safety Factor (minimum)	1.296	

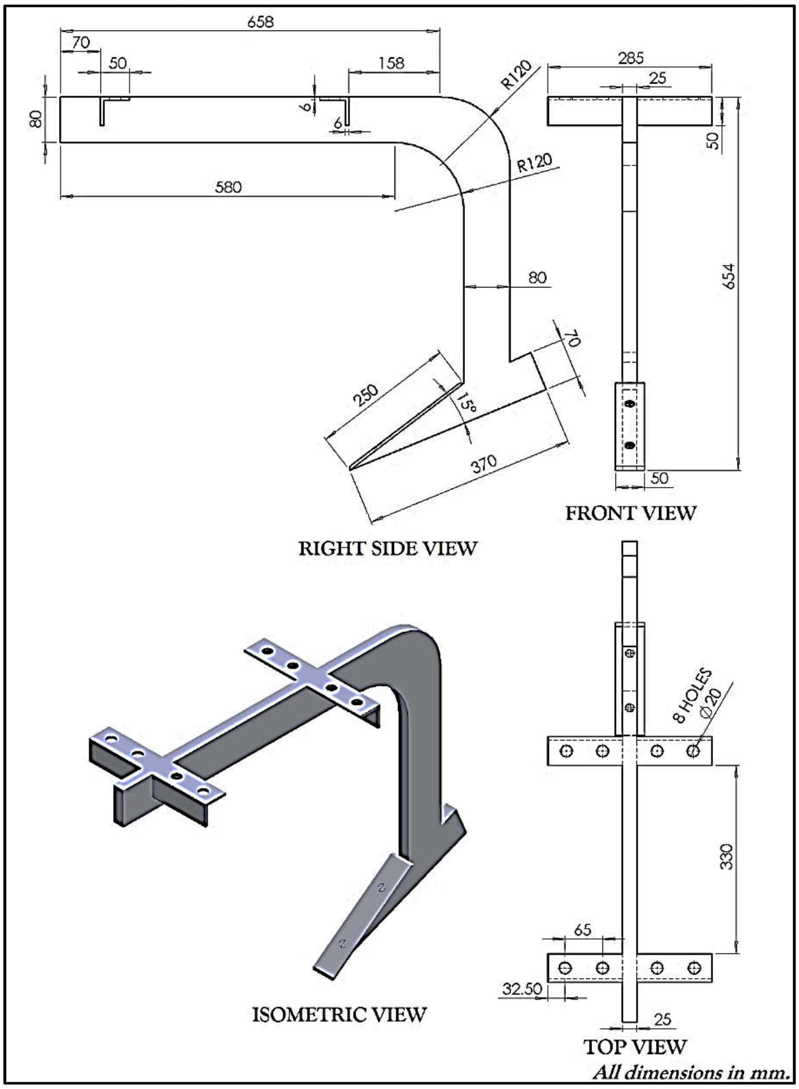

Fig. 5. Different views of the subsoiler

The maximum equivalent stress was lower than the material's yield stress (350 MPa), indicating that the design was safe. The results of the structural analysis are shown in Fig. 6.

3.3 Optimization

Results of the parametric correlation revealed that input parameters P1 and P3 impact the output parameters significantly, while the impact of input parameter P2 was negligible.

Table **3** shows the correlation of the input parameters with the output parameters obtained from DesignXplorer. P1 and P3 are termed as major input parameters with the best correlation values of 0.794 and -0.749 and R^2 values of 0.6304 and -0.5610 with P4 and P5. P2 is termed as a minor input parameter as the best correlation, and R^2 values are very low. P1 and P3 were chosen for further analysis, and P2 was ignored as it had a negligible effect on the output parameters.

In the Response Surface System, nine design points were generated according to the design module's design constraints. Results for all the output parameters of the subsoiler are included in the output from the DOE. Table 4 shows the various design sets and the variations in the output parameters due to variations in the input parameters.

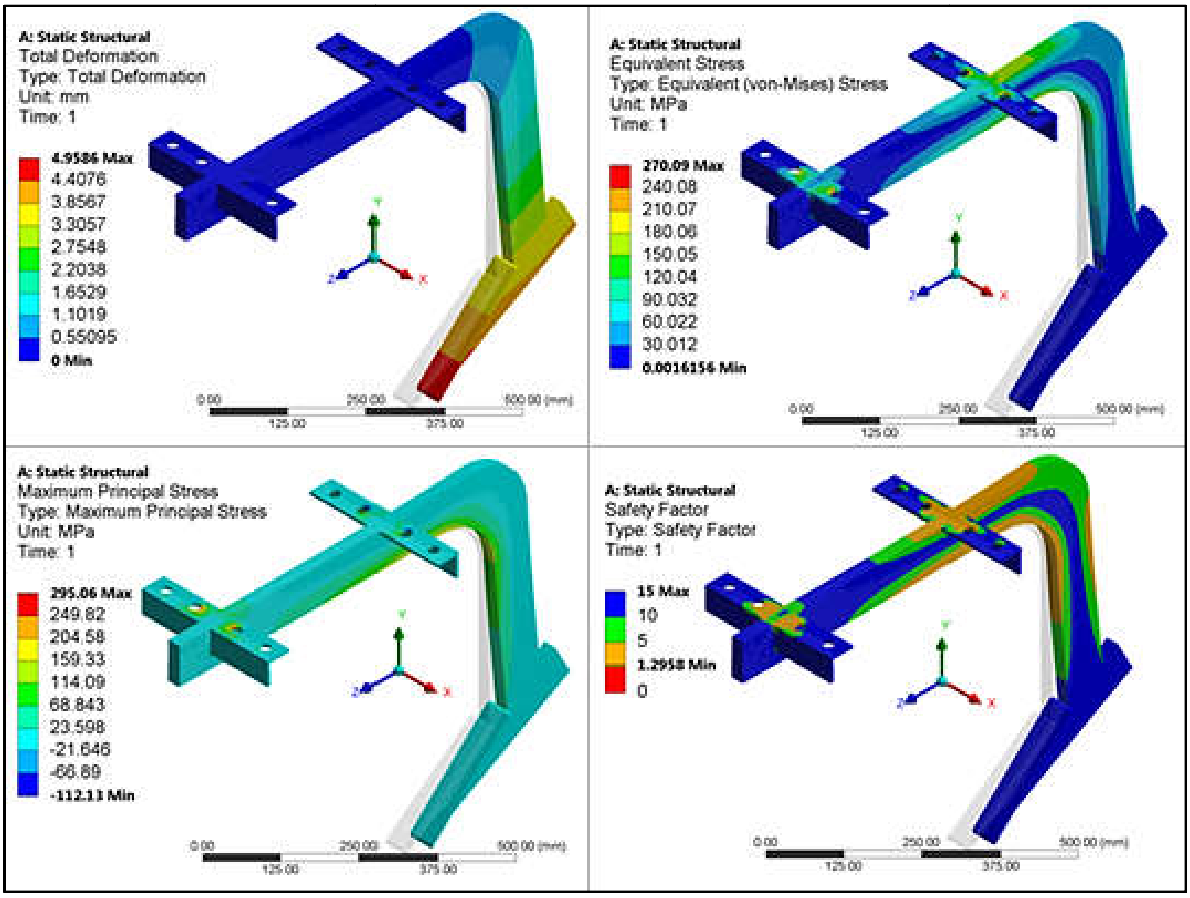

Fig. 6. Total deformation, equivalent stress, maximum principal stress and safety factor of the straight subsoiler obtained from the structural analysis

Table 3. Correlation between input and output parameters

	P4	P5	P6	P7	P8	P9
P1	0.794	-0.363	-0.609	-0.392	0.606	0.794
P2	0.044	-0.039	-0.123	-0.004	0.134	0.044
P3	0.460	-0.749	-0.650	-0.753	0.699	0.460

Table 4. Design points and the corresponding output parameters obtained from the design of experiments

Points name	Update order	P1	P3	P4	P5	P6	P7	P8	P9
1	5	22.50	80.00	20.26	3.98	249.46	279.47	1.40	2.57
2	2	20.00	80.00	18.33	4.45	266.59	300.02	1.31	2.33
3	8	25.00	80.00	24.54	4.96	270.09	295.06	1.30	3.12
4	4	22.50	70.00	19.14	5.15	315.86	332.84	1.11	2.43
5	6	22.50	90.00	21.37	3.22	245.86	280.62	1.42	2.72
6	1	20.00	70.00	17.34	5.77	354.88	375.28	0.99	2.20
7	7	25.00	70.00	20.95	4.66	311.06	325.73	1.13	2.66
8	3	20.00	90.00	19.32	3.61	268.16	287.87	1.31	2.45
9	9	25.00	90.00	23.43	2.91	226.28	255.05	1.55	2.98

Results from the Design of Experiments were used to generate Response surfaces both in 2D and 3D. Response surfaces showed that the straight subsoiler mass and volume increased with an increase in both the input parameters. The total maximum principal stress decreased as a result of the increase in the input parameters. The total deformation and equivalent stress decreased with the increase of P3, but the effect of P1 remained quite negligible. The safety factor increased with the increase of P3 but remained unaffected by the increase of P1. Results of the Response Surface System were further used in the optimization process. The results are generated as tradeoff charts and candidate points. The tradeoff charts between the input and output parameters are shown in Fig. 7.

The tradeoff charts revealed that the lowest safety factor value was 1.30, which corresponds to the initial design. It was noticed that the soil mass at this safety factor was 18.80 kg in comparison to the initial mass of 24.54 kg. This shows that the initial design was 5.74 kg (23.39%) overweight. The parameters P1 and P3 at this point were 20.19 mm and 77.83 mm, respectively. Raising the safety factor value to 1.40, the mass was 19.08 kg, 22.25% less than the initial design. The input parameters P1 and P3 were obtained as 20.058 mm and 86.26 mm, respectively.

The candidate points post-optimization are shown in Fig. 8. Each candidate point shows the input parameters and the corresponding output parameters. Candidate point 3 was the optimal choice among a set of one thousand sample points. Data from candidate point 3 was verified to check the solid model's suitability, and ANSYS simulation performed for agreement with the operating conditions. The optimized design parameters are listed in Table 5, and the final optimized design is shown in Fig. 9.

3.4 Comparison

A comparison of the subsoiler design with respect to both the input and output parameters was carried out. The changes between the initial and final design parameters is shown graphically in Fig. 10. The thickness of shank (P1), mass of subsoiler (P4), equivalent stress (P6), maximum principal stress (P7), and volume (P9) were reduced. The width of shank (P3), total deformation (P4), safety factor (P8) and minimum working life were increased. P1 reduced from 25 mm to 20 mm, P3 increased from 80 mm to 86.26 mm, P4 reduced from 24.54 kg to 20.89 kg, P5 increased from 4.9586 mm to 5.3133 mm, P6 reduced from 270.09 MPa to 259.02 MPa, P7 reduced from 295.06 MPa to

Table 5. Final design parameters for the optimized design

S. no.	Parameter	Value
1	P1 – Thickness of Shank (mm)	20.00
2	P3 – Width of Shank (mm)	86.26
3	P4 - Straight Subsoiler Mass (kg)	19.08
4	P5 - Total Deformation (mm)	3.76
5	P6 - Equivalent Stress (MPa)	250.4
6	P7 - Maximum Principal Stress (MPa)	293.65
7	P8 - Safety Factor	1.40
8	P9 - Straight Subsoiler Volume ($mm^3 \times 10^6$)	2.42

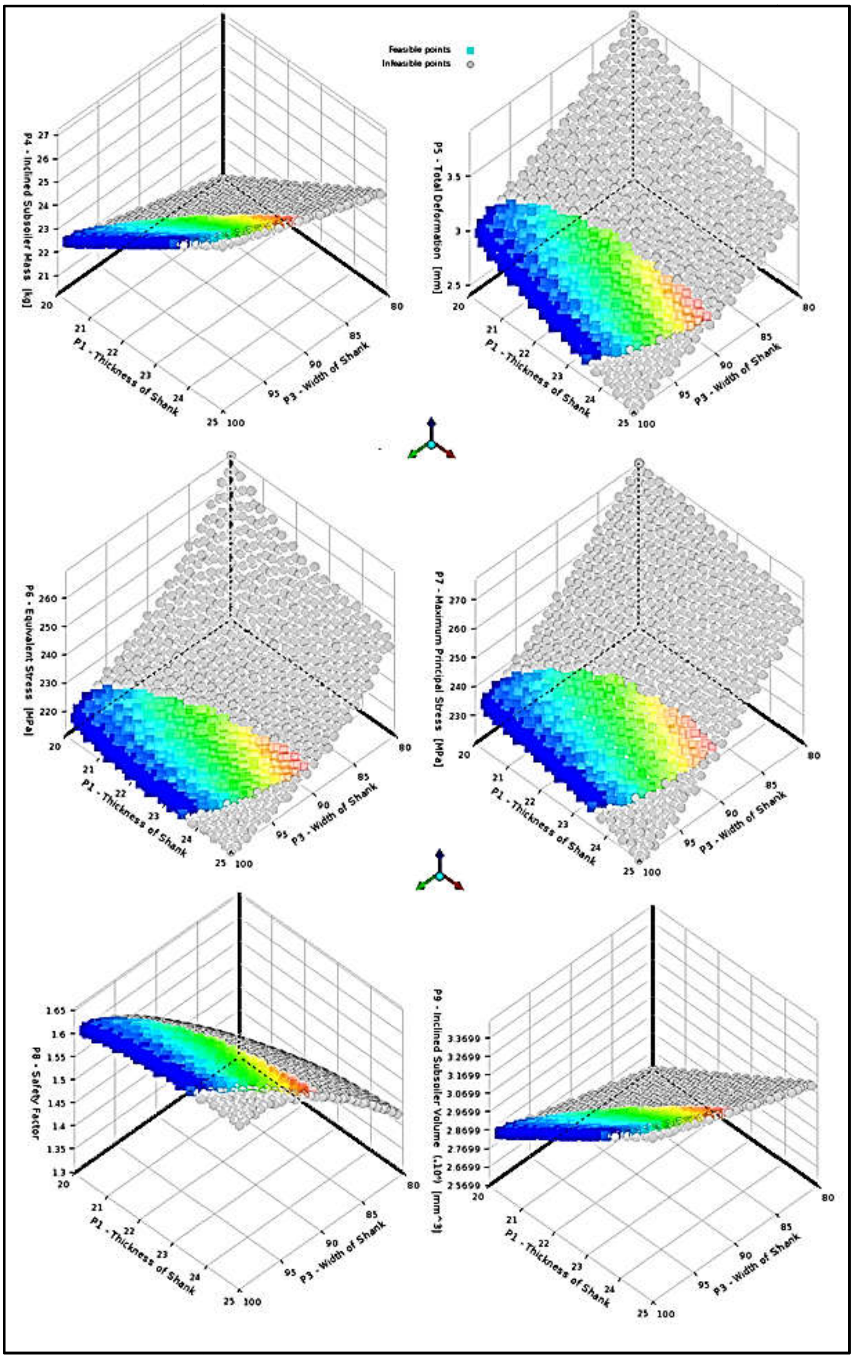

Fig. 7. Tradeoff charts of the output parameters

Schematic D4: Optimization , Candidate Points

A	B	C	D	E	F	G	H	I	J	K	L
Reference	Name	P1 - Thickness of Shank	P3 - Width of Shank	P4 - Straight Subsoiler Mass (kg)		P5 - Total Deformation (mm)	P6 - Equivalent Stress (MPa)	P7 - Maximum Principal Stress (MPa)	P8 - Safety Factor		P9 - Straight Subsoiler Volume (mm^3)
				Parameter Value	Variation from Reference				Parameter Value	Variation from Reference	
○	Candidate Point 1	20.078	88.76	★★ 19.132	0.26 %	3.4267	247.82	288.25	★ 1.4181	1.18 %	2.4303E+06
○	Candidate Point 2	20.038	87.51	★★ 19.089	0.03 %	3.5993	249.02	291.11	★ 1.4103	0.62 %	2.4248E+06
◉	Candidate Point 3	20.058	86.26	★★ 19.083	0.00 %	3.7639	250.4	293.65	★ 1.4016	0.00 %	2.4242E+06

Fig. 8. Candidate design points obtained after the optimization step

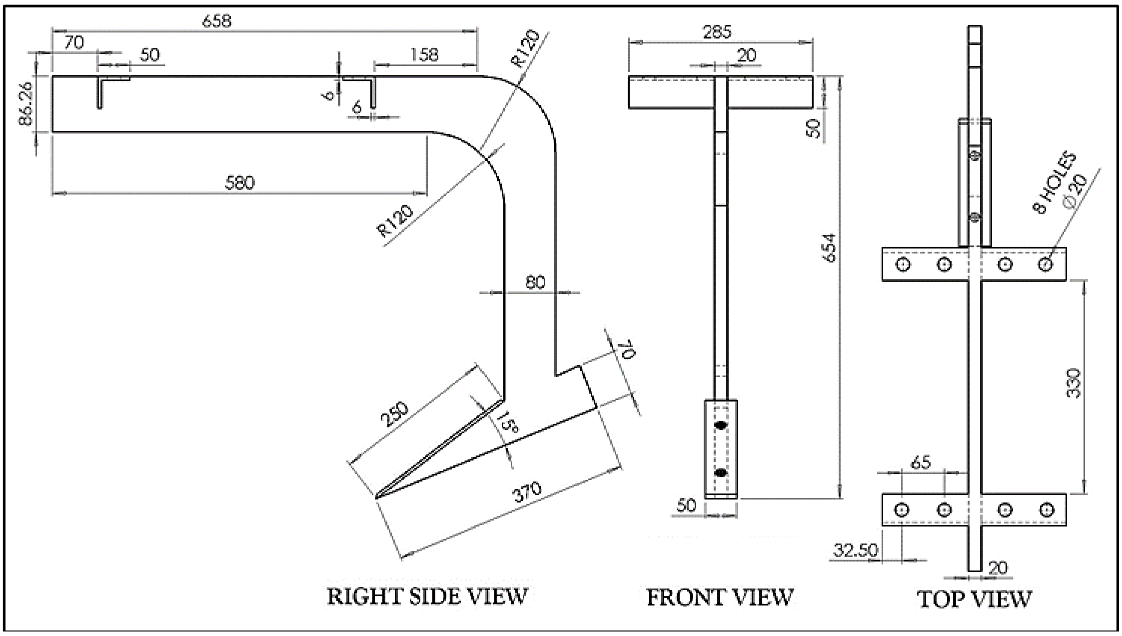

Fig. 9. Different views of the optimized subsoiler

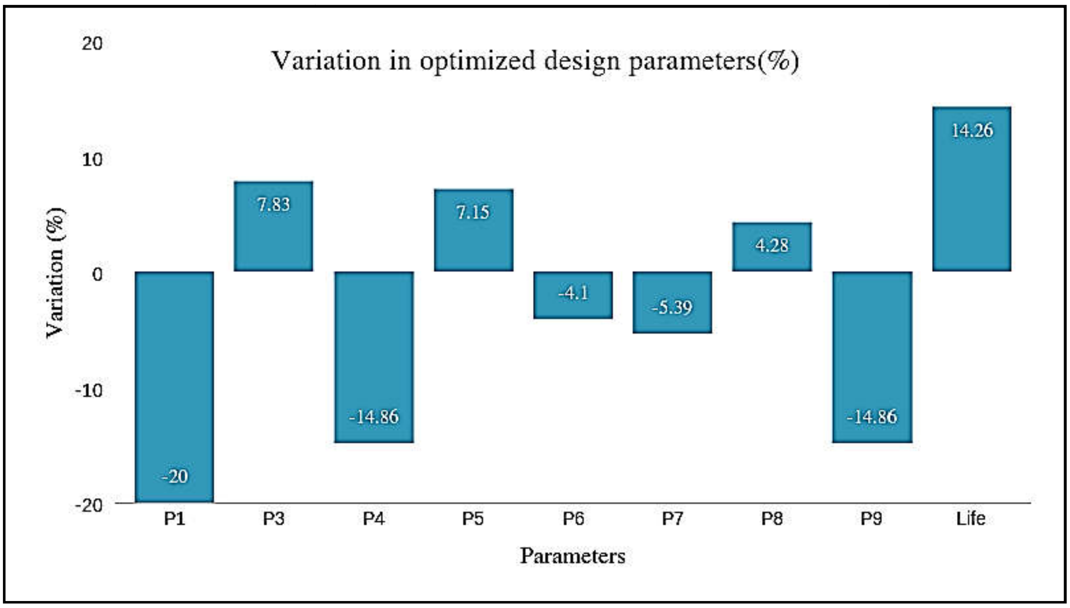

Fig. 10. Variation in optimized design as compared to the original design

279.16 MPa, P8 increased from 1.2958 to 1.3512, P9 reduced from 3.12×106 mm3 to 2.65×106 mm3 and the minimum working life increased from 9102.4 to 10400 cycles.

4. CONCLUSIONS

This study was performed for obtaining the optimum geometry parameters for a straight subsoiler using the finite analysis method. The 3D model was developed using SolidWorks 2016 software, and the structural optimization performed in the ANSYS software. Parametric correlation of the input and output parameters showed a strong relation of two input parameters -P1 and P3, with the output parameters. On the other hand, the relation between P2 and the output parameters was weak. Optimizing the straight subsoiler lowered the subsoiler mass and total volume by 14.86%. The maximum of both the equivalent stress and maximum principal stress were reduced by 4.10% and

5.39%, respectively, while the total deformation, minimum safety factor, and maximum working life were raised by 7.15%, 4.28%, and 14.26%, respectively.

The reduction in the subsoiler weight is profitable as it reduces the total production cost due to lesser material use. In addition to this, weight reduction also leads to a reduction in energy usage during its use as the equivalent energy for every kg of the agricultural machines is approximately 62.7 megajoules [32,33], and the lesser the weight, the lower is the energy consumption. Optimizing a machine using computer-aided design software thus helps in saving production costs by reducing the overuse of materials and reducing energy expenditure. Therefore, it can be concluded that the application of computer-aided design methods and optimization techniques, helps resource and energy conservation, together with the other advantages stated.

COMPETING INTERESTS

Authors have declared that no competing interests exist.

REFERENCES

1. Hamza MA, Anderson WK. Soil compaction in cropping systems: A review of the nature, causes and possible solutions. Soil Tillage Res. 2005. https://doi.org/10.1016/j.still.2004.08.009.
2. Gupta SC, Sharma PP, DeFranchi SA. Compaction Effects on Soil Structure. Adv Agron. 1989;42:311–38. https://doi.org/10.1016/S0065-2113(08)60528-3.
3. Whalley WR, Dumitru E, Dexter AR. Biological effects of soil compaction. Soil Tillage Res. 1995. https://doi.org/10.1016/0167-1987(95)00473-6.
4. BAKKEN LR, BØRRESEN T, NJØS A. Effect of soil compaction by tractor traffic on soil structure, denitrification, and yield of wheat (*Triticum aestivum* L.). J Soil Sci. 1987;38:541–52. https://doi.org/10.1111/j.1365-2389.1987.tb02289.x.
5. Akinci I, Cakir E, Topakci M, Canakci M, Inan O. The effect of subsoiling on soil resistance and cotton yield. Soil Tillage Res. 2004. https://doi.org/10.1016/j.still.2003.12.006.
6. Ozmerzi A. Mechanization of Garden Plants. Antalya, Turkey.: Akdeniz University Press; 2001.
7. Raper RL, Reeves DW, Schwab EB, Burmester CH. Reducing soil compaction of Tennessee Valley soils in conservation tillage systems. J Cott Sci. 2000;4(2):84–90.
8. Bluntzer JB, Ostrosi E, Niez J. Design for Materials: A New Integrated Approach in Computer Aided Design. Procedia CIRP. 2016;50:305–10. https://doi.org/10.1016/j.procir.2016.04.153.
9. Bogunovic I, Kisic I. Compaction of a Clay Loam Soil in Pannonian Region of Croatia under Different Tillage Systems. vol. 19. 2017.
10. Dan Wolf, Thomas H. Garner, Jack W. Davis. Tillage Mechanical Energy Input and Soil-Crop Response. Trans ASAE. 1981;24:1412–9. https://doi.org/10.13031/2013.34463.
11. A. Khalilian, T. H. Garner, H. L. Musen, R. B. Dodd, S. A. Hale. Energy for Conservation Tillage in Coastal Plain Soils. Trans ASAE. 1988;31:1333–7. https://doi.org/10.13031/2013.30866.
12. Dransfield P, Willatt ST, Willis AH. Soil-to-implement reaction experienced with simple tines at various angles of attack. J Agric Engng Res. 1964;9:220–4.
13. Topakci M, Celik HK, Canakci M, Rennie AEW, Akinci I, Karayel D. Deep tillage tool optimization by means of finite element method: Case study for a subsoiler tine. J Food, Agric Environ. 2010;8:531–6.
14. Kelley T. Optimization, an Important Stage of Engineering Design. Technol Teach. 2010;69:18.
15. Uzun YH. Optimization Techniques in Mechanical Engineering. Yildiz Technical University, 2006.
16. Vanderplaats GN. Structural optimization for statics, dynamics and beyond. J Brazilian Soc Mech Sci Eng. 2006;28:316–22. https://doi.org/10.1590/S1678-58782006000300009.
17. Jayasuriya HPW, Salokhe VM. A review of soil-tine models for a range of soil conditions. J Agric Eng Res. 2001;79:1–13. https://doi.org/10.1006/jaer.2000.0692.
18. Gupta C, Marwaha S, Manna M. Finite element method as an aid to machine

design: A computational tool. Excerpt from Proc. COMSOL Conf. 2009, Bangalore., 2009.
19. Gu S. Application of finite element method in mechanical design of automotive parts. IOP Conf. Ser. Mater. Sci. Eng., vol. 231, Institute of Physics Publishing; 2017. https://doi.org/10.1088/1757-899X/231/1/012180.
20. Hong L, Jianrong Z. Application of Agriculture Machinery Digitized Design and Manufacture Technology [J]. Agric Equip Technol. 2007;6.
21. Al-Kheer AAKA. Integrating the concepts of optimization and reliability in the design of agricultural machines. 2010.
22. Tao Z. Optimization of Steel Storage Rack Pothook Hole Base on ANSYS Workbench. IJRES. 2018;6:14–9.
23. Alavala CR. Finite element methods: Basic concepts and applications. PHI Learning Pvt. Ltd.; 2008.
24. IS:2062-E250. Hot rolled medium and high tensile structural steel — Specifications. 2011.
25. Madenci E, Guven I. The finite element method and applications in engineering using ANSYS®. Springer; 2015. https://doi.org/10.1007/978-1-4899-7550-8.
26. Delfel S. Introduction to Mesh Generation with ANSYS Workbench. Coanda research and development corporation; 2013.
27. Vedaprabha HC, Ali H. Stress and Deformation Analysis of Accelerated Pedal Mechanism. Int J Eng Manag Res. 2015;5:364–9.
28. Yadav M V. Force and pressure distribution on selected tillage machinery. M. Tech. dissertation (unpublished), Banda University of Agriculture, 2014.
29. Ajit K. Srivastava, Carroll E. Goering, Roger P. Rohrbach, Dennis R. Buckmaster. Chapter 8 Soil Tillage. Eng. Princ. Agric. Mach. Second Ed., St. Joseph, MI: American Society of Agricultural and Biological Engineers; 2006, p. 169–230. https://doi.org/10.13031/2013.41470.
30. Pelegri AA, Tekkam A. Optimization of laminates' fracture toughness using design of experiments and response surface. J Compos Mater. 2003. https://doi.org/10.1177/002199803029748.
31. Bhatia V, Karthikeyan R, Ganesh Ram RK, Cooper YN. Design optimisation and analysis of a quadrotor arm using finite element method. Appl. Mech. Mater., 2014. https://doi.org/10.4028/www.scientific.net/AMM.664.371.
32. Mohansing J. On farm energy use pattern in different cropping systems in Haryana. India. International Institute of Management-University of Flensburg, 2002.
33. De D, Singh RS, Chandra H. Technological impact on energy consumption in rainfed soybean cultivation in Madhya Pradesh. Appl Energy. 2001;70:193–213. https://doi.org/10.1016/S0306-2619(01)00035-6.

© 2020 Allaie et al.; This is an Open Access article distributed under the terms of the Creative Commons Attribution License (http://creativecommons.org/licenses/by/4.0), which permits unrestricted use, distribution, and reproduction in any medium, provided the original work is properly cited.

Peer-review history:
The peer review history for this paper can be accessed here:
http://www.sdiarticle4.com/review-history/62159